Catal Lett (2007) 117:53–61
DOI 10.1007/s10562-007-9150-5

Powder and Monolith-Supported Sulphur Trap Materials Based on Modified Hydrotalcite-Derived Supports

Ellen Schreier · Reinhard Eckelt · Manfred Richter · Rolf Fricke

Received: 15 May 2007 / Accepted: 3 June 2007 / Published online: 22 June 2007

Abstract SO_x traps were prepared using hydrotalcite materials of different composition and their SO_x storage properties were monitored during temperature cycling (50–600 °C) under continuous feed streams (50 ppm SO_2, 6 vol.% O_2, 5 vol.% CO_2, 100 ppm NO) at a space velocity of 144,000 L/(kg h). A comparison is made with non-hydrotalcite mixed oxide supports as well as pure alumina. The most promising material $NaMnO_x/Al_2O_3$ was wash-coated on a cordierite core and its SO_x trap capacity was compared with the performance of the powder and the slurry. The slurry as well as the monolith-supported material showed an SO_2 uptake of 93% over 7 h time-on-stream corresponding to 20 wt.% sulphate. DRIFT spectroscopy revealed the prevailing sulphate formation on Mn-related sites and Na. Regeneration of the trap with CO/H_2 ($\lambda = 0.99$) at 600 °C was not completely possible.

Keywords Sulphur trap · SO_x trap · Hydrotalcite · Manganese · Alkali metals · Monolith

1 Introduction

Operating gasoline-powered Otto engines under lean-burn conditions decrease fuel consumption and hence CO_2 emissions. However, the common three-way catalyst (TWC) is unable to reduce NO_x to molecular nitrogen, because the exhaust contains high oxygen concentrations under lean conditions.

E. Schreier · R. Eckelt · M. Richter (✉) · R. Fricke
Leibniz Institute for Catalysis, Branch Berlin (former ACA), P.O. Box 961156, 12474 Berlin, Germany
e-mail: manfred.richter@catalysis.de

One promising approach for NO_x reduction under oxygen excess is the NO_x-storage-reduction (NSR) concept. Principally, NSR catalysts are TWCs, modified by a NO_x storage component (alkali, earth alkali or rare earth metals). NO_x is stored as nitrate under lean conditions. Conversion of nitrates is achieved onboard by short rich fuel excursions [1–4]. At this operation window ($\lambda \approx 1$) nitrates are decomposed and NO_x is reduced to N_2 by the TWC function.

Sensitivity against poisoning by SO_2/SO_3 originating from fuels or lubricants is a drawback of the current NSR catalysts. Sulphates are formed with the storage components [5]. These sulphates possess higher thermal stability than nitrates, and the NO_x storage capacity progressively declines by accumulation of stable sulphates leading to a continuous deactivation of the catalyst [1, 6–8].

Reactivation of the sulphated NSR catalyst is difficult yet possible [9–13], but causes additional fuel consumption thus decreasing the benefit of lean operation.

One alternative is to protect the NSR catalyst by an upstream placed SO_x trap [14–18]. The SO_x storage capacity of the trap should be as high as possible to enable replacement during regular inspection intervals of the vehicles. Otherwise, onboard regeneration is required with bypassing of the NSR catalyst.

Several materials have been shown to possess properties for SO_2 adsorption from exhaust streams such as perovskites ($BaSnO_3$) [19], Na/γ–Al_2O_3 [20], MgO powder [21], different zeolite structures (MCM-22, MCM-36, ITQ-2) loaded with Ba, Al, Mg, Pt, Cu [15], manganese-containing materials in various compositions and structures, e.g. octahedral molecular sieves (OMS) [22], mixed supported oxides, e.g. $NaMn/Al_2O_3$–CaO [16, 18] or MnO_x–CeO_2 mixed oxides [23].

Hydrotalcites (layered double hydroxides, LDH) are regarded as suitable base materials for the development of

NO_x as well as of SO_x traps [24–33]. Their exchangeable interlayer anions like Cl^-, NO_3^-, OH^-, SO_4^{2-} [34, 35] are supposed to offer space accessible for SO_x storage.

The question not adequately addressed so far is whether the stability of the hydrotalcite supports is high enough to allow onboard regeneration of the SO_x trap taking place at temperatures as high as 600 °C. Moreover, results are missing about the effects of wash-coating the powdered materials on monoliths for application in automotives.

These two aspects were examined. SO_x traps were prepared using hydrotalcite materials of different composition and their SO_x storage properties were monitored during temperature cycling. A comparison is made with non-hydrotalcite mixed oxide supports as well as pure alumina. The most promising material was coated on a cordierite core and its SO_x trap capacity was compared with the performance of the powder.

2 Experimental

2.1 Materials

Powdered samples were prepared by precipitation of an amorphous MnO_x phase in the presence of suspended hydrotalcite powders $[Mg_{1-x}Al_x(OH)_2(CO_3)_{x/2}yH_2O$ (Pural/Sasol) with different $MgO:Al_2O_3$ ratios of 30:70 (MG30), 50:50 (MG50) and 70:30 (MG70), mesoporous mixed Al_2O_3–MgO oxides as well as mesoporous Al_2O_3.

Hydrotalcites were used as delivered, but sieved to a particle fraction below 200 µm before modification. Mesoporous Al_2O_3–MgO ($MgO:Al_2O_3$ = 30:70) was prepared from a solution of 84 g Al-sec.-butylate (solved in 200 g propanol-2) and an aqueous solution of Mg acetate (40 g). A solution of 12 g $(NH_4)_2CO_3$ in 50 mL H_2O was added to avoid fast precipitation of $Mg(OH)_2$. After filtering the precipitate was dried at 120 °C. Before further use the materials were additionally calcined at 600 °C for 1 h. The support is denoted as EMG30.

For the synthesis of an Al_2O_3 support 102 g Al-sec.-butylate was solved in 300 g propanol-2 and 30 g H_2O. After 30 min stirring the product was filtered, dried at 120 °C and finally calcined at 500 °C for 1 h.

Precipitation of a nonstoichiometric MnO_x ($x < 24$) phase was achieved by reaction (1)

$$3Mn^{2+} + 2MnO_4^- + 2H_2O \rightarrow 5MnO_2 \downarrow + 4H^+ \quad (1)$$

using solutions of Mn(II) acetate and $KMnO_4$ [36]. After adjustment of the pH value to nearly seven by addition of NH_3, the suspensions were heated to 80 °C, kept for further 30 min at this temperature and then filtered, dried and finally calcined at 600 °C for 1 h. The target MnO_x concentration on these supports was about 20 wt.%.

Selected samples were additionally impregnated with a solution of Na_2CO_3 to obtain 10 wt.% Na loading.

Characterization data of all samples are given in Table 1. The samples are denoted according to their oxidation/storage components and the kind of support, e.g. $NaMnO_x$/EMG30 means a material where the EMG30 support was modified by the MnO_x phase and additionally by impregnation with a Na solution.

Monolith samples were prepared from the most promising powder material, viz. $NaMnO_x/Al_2O_3$. Monolith cores with a dimension of 1.0 × 1.378 inch (17.7×10^{-3} L) were drilled out from a cordierite honeycomb substrate having a wall thickness of 8 mil (≈0.20 mm) and a cell density of 300 cells/in^2. A slurry was made from the powder sample by dispersing it in an aqueous solution containing polyvinyl alcohol as binder. The cores were dipped in this slurry several times with intermediate drying at 120 °C. Final calcination was performed at 400 °C in air for 1 h to ensure decomposition of the polyvinyl alcohol. Composition and textural values of the used slurry are shown in Table 1.

The loading of the monolith with the MnO_x storage material was about 17 wt.%. After calcination at 400 °C for 1 h the monolith was additionally impregnated with the Na_2CO_3 solution, dried at 120 °C for 1 h and finally calcined at 500 °C for 1 h. After this procedure all channels were still accessible.

2.2 Characterization

The chemical composition of the samples was determined by optical emission spectroscopy with excitation by inductively coupled plasma (OES-ICP) using the spectrometer Optima 3000 XL (Perkin Elmer).

Pore volume and surface area were determined by nitrogen adsorption on an ASAP 2010M facility (Micromeritics).

DRIFT measurements were performed on the FTS-60 A spectrometer (BIO-RAD) by using a diffuse reflectance attachment (HARRICK) equipped with a reaction chamber that allows heating under gas flow from room temperature to 500 °C. A number of 256 single beam spectra were co-added at a resolution of 2 cm^{-1}. The spectra are presented as Kubelka-Munk function referred to the adequate background spectra (samples are recorded at same temperatures in He/O_2). A feed containing 50 or 200 ppm SO_2 and 5 vol.% O_2 in He was used in the temperature range between 25 and 500 °C.

2.3 Temperature Programmed Adsorption and Desorption Experiments of SO_2 (SO_x TPA/D)

TPA/D studies on the powdered SO_x trap materials were carried out in a flow system equipped with an integral flow

Table 1 Characterization of investigated SO_x trap materials

Storage material	Calc. temp (°C)	Composition (%)	BET (m^2/g)	Pore vol. (cm^3/g)
PURAL MG30[a]	–	39.96 Al, 14.77 Mg	271[a] (250)	(0.533)
MnO_x/MG30	600	23.08 Al, 11.38 Mg, 16.62 Mn	177	0.467
$NaMnO_x$ /MG30	600	19.95 Al, 9.40 Mg, 14.05 Mn, 9.54 Na, 2.19 K[b]	95	0.308
PURAL MG50[a]	–	29.19 Al; 27.04 Mg	228[a] (211)	(0.236)
MnO_x/MG50	600	16.74 Al; 18.76 Mg, 16.39 Mn;	162	0.369
PURAL MG70[a]	–	18.14 Al; 39.63 Mg	201[a] (166)	(0.286)
MnO_x/MG70	600	10.96 Al, 26.34 Mg, 16.65 Mn,	130	0.311
EMG30 (Al_2O_3–MgO)[c]	600	35.4 Al, 16.9 Mg	325	0.640
Na/EMG30	600	29.7 Al. 14.0 Mg. 10.9 Na	86	0.222
MnO_x/EMG30	600	Not det.	227	0.561
$NaMnO_x$/EMG30	600	21.4 Al. 10.0 Mg. 16.1 Mn. 10.0 Na. 1.3 K[b]	97	0.339
Al_2O_3	600		305	1.079
Na/Al_2O_3	600	44.3 Al. 10.1 Na	156	0.608
MnO_x/Al_2O_3	600	Not det.	225	0.517
$NaMnO_x$/Al_2O_3	600	30.0 Al, 16.5 Mn, 9.1 Na, 2.2 K[b]	114	0.346
$NaMnO_x$/Al_2O_3 dried slurry	400	28.2 Al, 10.8 Mn, 9.7 Na, 1.1 K[b]	121	0.218

[a] Data from Sasol Germany GmbH (after activation for 3 h at 550 °C), values in parenthesis redetermined (after calcination at 600 °C for 1 h) before modification

[b] Potassium is introduced by the MnO_x loading using $KMnO_4$ and $Mn(CH_3COO)_2$ solution (see text)

[c] EMG30 is an Al_2O_3–MgO support (synthesis of LIKAT) with a similar composition like PURAL MG30 but without possessing the hydrotalcite structure (after calcination at 600 °C for 1 h)

reactor (internal diameter 10 mm) and an on-line sampling system. The composition of the exit stream (SO_2, CO_2, and O_2) was continuously analyzed by a Maihak Multigas sensor. A condenser located in front of the multigas sensor was used when the feed contained water. The SO_x TPA/D was performed with 50 mg of the storage materials starting the experiment at 50 °C. Applying the so-called 'cyclic mode' [18] the reactor temperature was linearly increased and decreased between 50 and 600 °C with a heating rate of 10 K/min. One cycle comprised a temperature increase from 50 to 600 °C followed by a decrease to 50 °C. Usually, four cycles were applied to complete a test run under a continuous feed (flow rate 120 cm^3/min) composed of 50 ppm SO_2, 6 vol.% O_2, 5 vol.% CO_2 balanced by He. In some cases 100 ppm NO and/or 7 vol.% H_2O was added to the feed.

The concentration versus temperature profiles indicate adsorption/desorption of SO_2 if the outlet concentration of SO_2 is lower/higher than the inlet concentration. The amounts of stored SO_2 were determined by integration of the corresponding areas of the profiles and a storage capacity was calculated referring to the inlet molar flow for the considered time-on-stream.

TPA/D studies on the monolithic SO_x trap was performed in a quartz tube flow reactor system with on line coupled mass spectrometric analysis (Omnistar, Pfeiffer Vacuum). The monolith core was placed into the horizontally arranged reactor and was gas-tightened against the glass wall by a quartz wool tape. Two thermocouples were directly placed in front and behind the monolith, allowing the determination of temperature gradients over the sample length. To avoid analytical artefacts by secondary gas phase reactions in the free reactor volume the inlet capillary of the mass spectrometer was positioned right behind the monolith sample.

The feed gas composition was the same as used for tests of the powder samples. To keep equivalent space velocities, a flow rate of 4 L/min was applied for the monolith material. In both cases the gas hourly space velocity (GHSV), referred to the powder, amounted to about 144,000 L/(kg h).

3 Results and Discussion

3.1 Powder Samples

Results for hydrotalcite-based SO_x trap materials MnO_x/MG30, MnO_x/MG50, and MnO_x/MG70 are shown in Fig. 1. It can be seen, that the removal efficiency for SO_2 achieved 80–100% at cycle maximum temperature (600°C) with no significant differences between the samples during the first cycle (0–125 min time-on-stream). During the following three temperature cycles, the performance

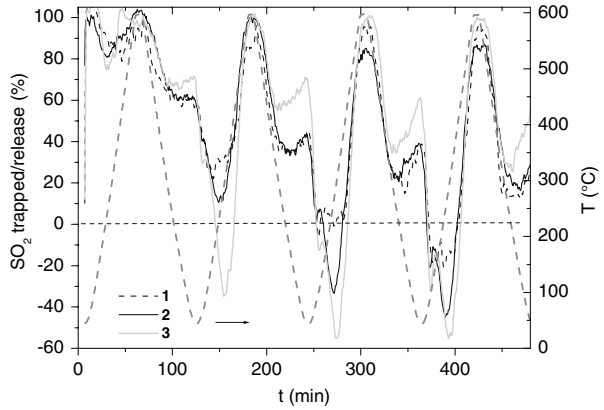

Fig. 1 SO_2 uptake of MnO_x on different hydrotalcites: (1) MG30, (2) MG50, (3) MG70. SO_x TPA/D in feed atmosphere from 50 to 600 °C (temperature ramp 10 K/min; intermediate cooling from 600 to 50 °C, dashed grey line, right axis), feed: 50 ppm SO_2. 6 vol.% O_2, 5 vol.% CO_2, balance He

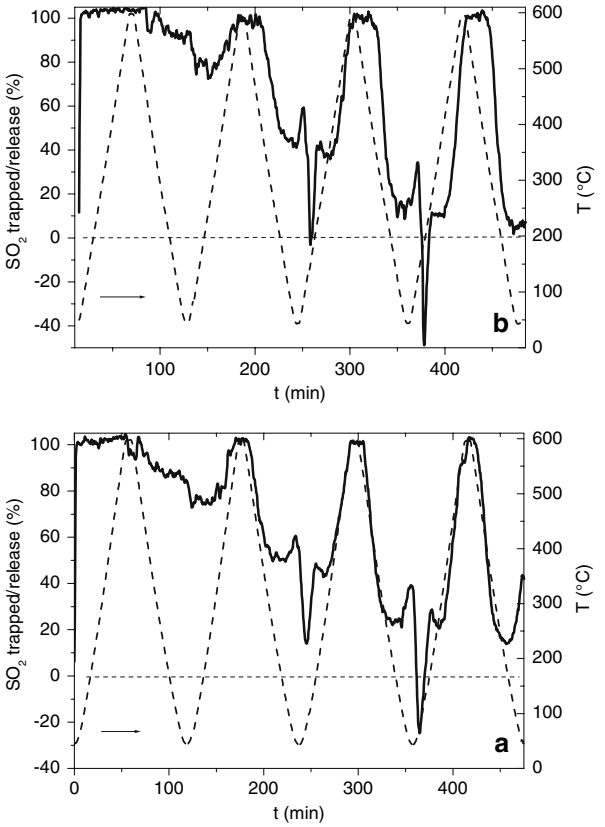

Fig. 2 SO_2 uptake of MnO_x on non-hydrotalcite supports (**a**) EMG30 and (**b**) Al_2O_3. TPA/D in feed atmosphere from 50 to 600 °C (temperature ramp 10 K/min; intermediate cooling from 600 to 50 °C, dashed line, right axis), feed: 50 ppm SO_2. 6 vol.% O_2, 5 vol.% CO_2, balance He

gradually decreases with some different behaviour of the samples. Obviously, temperature cycling under $SO_2/O_2/CO_2$ modifies the structure of the SO_x trap. It can be concluded that MnO_x/MG30 shows the most favourable properties of the hydrotalcite-based samples. The minimum of the SO_2 storage-versus-time profile does not coincide with the lowest temperature (50 °C) but is achieved at the ascending side of the temperature cycle at about 200–300 °C. Because the SO_2 concentration at the reactor outlet is higher than at the inlet, weakly fixed, physisorbed SO_2 is obviously released.

The corresponding SO_2 storage test results for MnO_x/EMG30 and MnO_x/Al_2O_3 are shown in Fig. 2a and b, respectively. The SO_2 storage-versus-time profiles during temperature cycling are comparable to those of MnO_x/MG30 (Fig. 1), i.e. 100% SO_2 storage is achieved at 600 °C. The lowest net storage of SO_x is observed between 100 and 200 °C due to desorption of weakly fixed, physisorbed SO_2. The SO_2 storage capacity averaged over the four cycles (referred to the offered amount of SO_2) reached 65% for sample MnO_x/EMG30, corresponding to 16 wt.% of sulphate. Roughly, the same value for the overall storage capacity (66%) was obtained for sample MnO_x/Al_2O_3, where the support contained no MgO (Fig. 2b).

In summary, comparing the investigated MnO_x/support materials, it seems obvious that the use of hydrotalcite supports did not show any advantage over non-hydrotalcite Al_2O_3–MgO under the experimental conditions applied. Moreover, MgO-free Al_2O_3 is an equivalent support.

It can be concluded that the hydrotalcite structure has been destroyed during temperature cycling. It is known, that the hydrotalcite structure is not stable at higher temperatures [34, 35]. For Al/Mg hydrotalcite samples of a similar MgO:Al_2O_3 ratio like MG50 and MG70, Rey et al. [34] reported that already at 300 °C a process of dehydroxylation and decarbonation of the hydrotalcites starts, which simultaneously lead to an increase of specific surface area and pore volume. Gradual destruction of the layer structure is reported if the calcination temperature was increased with final transformation into MgO and $MgAl_2O_4$ at about 800 °C. Formation of the same oxides were observed by Di Cosimo et al. [35] after decomposition of hydrotalcite precursor materials at 400 °C in nitrogen.

XRD measurements of the calcined hydrotalcite samples (not shown) revealed that the intensities of the diffraction lines characterizing the hydrotalcite structure dramatically decreased after calcination at 600 °C but no diffraction lines of crystalline MgO or $MgAl_2O_4$ appeared.

Further experiments concentrated on the use of non-hydrotalcite support EMG30 and Al_2O_3 with the aim to improve the performance. It could be shown recently [18] that further modification of this type of storage material with about 10 wt.% Na enhanced the SO_2 uptake, particularly in the lower temperature range. Therefore, the influence of Na addition was tested using the EMG30 and

Table 2 SO_2 uptake results (cyclic mode) of modified Al_2O_3–MgO (EMG30) and Al_2O_3 supports

Material	SO_2 removal[a] (%)	SO_4^{2-} trapped (wt.%)
Al_2O_3	36	8.8
Na/Al_2O_3	55	13.6
MnO_x/Al_2O_3	66	16.3
$NaMnO_x/Al_2O_3$	83	20.4
$NaMnO_x/Al_2O_3$ (dried slurry)	72	18
EMG30	29	7.1
Na/EMG30	63	15.5
MnO_x/EMG30	65	16.2
$NaMnO_x$/EMG30	67	15

[a] SO_2 removal is referred to the overall SO_2 offering during four temperature cycles

Al_2O_3 supports. Figure 3 shows the results. Numerical values are summarized in Table 2.

The supports EMG30 and Al_2O_3 adsorb SO_2 at low temperature but release it completely at higher temperature. This shows that the ability of the non-modified supports to store SO_x as sulphate is quite low. The major part of the adsorbed SO_2 is probably only weakly physisorbed.

As already shown in Fig. 2, the modification of EMG30 and Al_2O_3 with MnO_x distinctly increased the ability of the material to store SO_x, i.e. Mn fulfils a two-fold task, viz. (i) it oxidizes SO_2 to SO_3 and (ii) it stores SO_3 as sulphate. Surprisingly, modification of the supports with sodium shows a similar effect of enhanced storage of SO_x as modification with MnO_x (see Fig. 3a, b). It should be noted that this effect occurs without the presence of an oxidation component, which is usually regarded as a necessary condition for oxidation of SO_2 to SO_3 and subsequent storage. It is known, however, that activated sodium carbonate (Na_2CO_3) effectively reacts with adsorbed SO_2 to form Na_2SO_3 already at low temperature [37]. In the presence of oxygen and at higher temperatures part of Na_2SO_3 can also be transformed into Na_2SO_4, that is very stable. Therefore, it is concluded that on Na/EMG30 and Na/Al_2O_3, sodium carbonate forms by reaction of the modifier Na with CO_2, which is a feed component, followed by reaction with SO_2 as described in Ref. [37].

The modification of the two supports with both Na and MnO_x further improved the SO_2 storage effect (Fig. 3). The most promising sample of this type of material is $NaMnO_x/Al_2O_3$, which stored about 20 wt.% sulphate within four temperature cycles at an average degree of SO_2 removal of about 80% under the applied conditions (cf. Table 2).

To cover the possible competition between SO_2 and NO for the same sites on the trap material the influence of NO has been investigated on sample $NaMnO_x/Al_2O_3$. The SO_x storage behaviour is not significantly affected by the

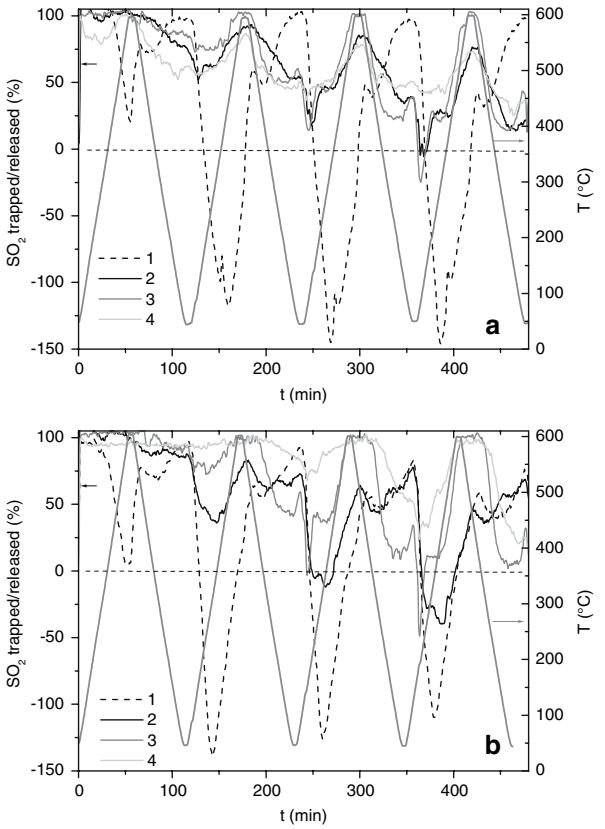

Fig. 3 SO_2 uptake (**a**) on sample EMG30 (1), Na/EMG30 (2), MnO_x/EMG30 (3), and $NaMnO_x$/EMG30 (4); (**b**) on Al_2O_3 (1), Na/Al_2O_3 (2), MnO_x/Al_2O_3 (3), and $NaMnO_x/Al_2O_3$ (4). TPA/D in feed atmosphere from 50 to 600 °C (temperature ramp 10 K/min; intermediate cooling from 600 to 50°C, grey line, right axis), feed: 50 ppm SO_2. 6 vol.% O_2, 5 vol.% CO_2, balance He

presence of NO (Fig. 4a, b). Nevertheless, some fluctuation of the NO concentration and hence its storage is observed. NO is adsorbed to a great extent at low temperatures, but nearly completely desorbed if the temperature reached higher values (Fig. 4b). However, the adsorption–desorption amplitude of temporal NO storage and desorption decreased with ongoing cycling. Clearly, SO_2 storage is the dominating effect on the material and competitive simultaneous NO_x storage is comparatively small.

Recent results, that addition of water to the feed has no negative effect on the SO_x uptake [18], could be confirmed for the $NaMnO_x/Al_2O_3$ material.

This $NaMnO_x/Al_2O_3$ material (30% Al, 16.5% Mn, 9.1% Na, 2.2% K) was chosen for wash-coating the monolith (see Sect. 3.3).

3.2 DRIFT Spectroscopy

In-situ DRIFT spectra of various powder samples during exposure to SO_2 (200 ppm)/O_2 (7.4 vol.%) at 100 °C are displayed in Fig. 5. Spectra for sample MnO_x/Al_2O_3 are

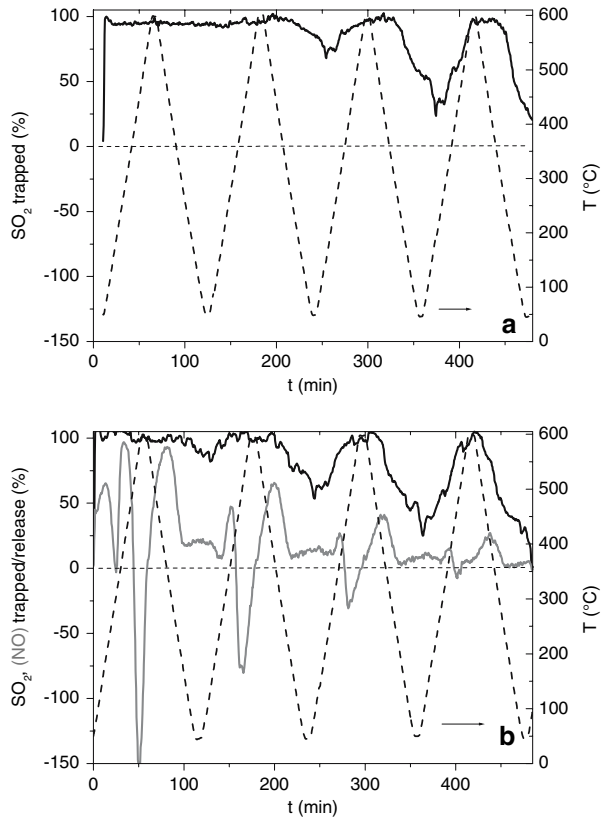

Fig. 4 SO_2 uptake on $NaMnO_x/Al_2O_3$ without NO (**a**) and with 100 ppm NO in the feed (**b**). TPA/D in feed atmosphere from 50 to 600 °C (temperature ramp 10 K/min; intermediate cooling from 600 to 50 °C, dashed line, right axis), feed: 50 ppm SO_2. 6 vol.% O_2, 5 vol.% CO_2, 100 ppm NO (only **b**), balance He

shown in dependence on time-on-stream (Fig. 5a) whereas properties of Al_2O_3, Na/Al_2O_3,MnO_x/Al_2O_3, and $NaMnO_x/Al_2O_3$ after 30 min exposure to the feed at 100 °C are compared in Fig. 5b.

On MnO_x/Al_2O_3 (Fig. 5a) two bands appeared at 1,280 and 1,180 cm^{-1} after 20 min time-on-stream. The band intensities increased with time-on-stream while a slight shift of wave numbers is observed to 1,295 and 1,190 cm^{-1}, respectively. Practically, a steady state is achieved after 60 min time-on-stream. These observed bands can be attributed to overlapping absorption of sulphate species on Mn, Al and K sites. Kijlstra et al. [38] assigned bands at 1,370 and 1,100 cm^{-1} to $(Al–O)_3S=O$ species and bands at 1,350 and 1,180 cm^{-1} to sulphate species on Mn loaded MnO_x/Al_2O_3 materials. The wave number of the bands depends on the temperature treatment of the samples. The shift of band positions seems to reflect the (partial) conversion of surface species to bulk species at increasing temperature.

No IR band could be observed on Al_2O_3 (Fig. 5b) confirming the result of the storage test where no significant SO_2 uptake had been found (Fig. 3b). A broad band of low intensity centred at about 1,180 cm^{-1} is observed in the spectrum of sample Na/Al_2O_3, which is tentatively assigned to sulphate formed on Na sites. Na_2SO_4 absorption bands are also found in this region [16].

Besides the band at 1,180 cm^{-1} the spectrum of sample MnO_x/Al_2O_3 shows an additional band at 1,280 cm^{-1} which is suggested to be caused by sulphate species on Mn sites. In an additional experiment the stability of these bands has been tested by treating the sample with a gas mixture of 10 vol.% H_2 in He in the temperature range 50–500 °C. The intensity of the two bands did not change during this treatment showing high stability of the appropriate sulphate species up to 500 °C.

The spectrum of $NaMnO_x/Al_2O_3$ shows a very intense absorption between 1,350 and 1,050 cm^{-1} with a maximum at 1,180 cm^{-1}. Obviously, the IR absorption in this region is an overlap of different bands, which could not be resolved. However, bands at 1,180 and 1,280 cm^{-1} represent a major contribution. Because the band at 1,280 cm^{-1} has only been observed in the presence of MnO_x, it is assigned to sulphate formation similar to $MnSO_4$. The assignment of the band at 1,180 cm^{-1} is more difficult because Na and K (originating from the preparation of the MnO_x phase) as well as Al are able to form sulphates. However, due to the absence of this band on the pure Al_2O_3 sample and the high concentration of alkali metals (9.1 wt.% Na and 2.2 wt.% K) of sample $NaMnO_x/Al_2O_3$, the band at 1,180 cm^{-1} should mainly indicate the existence of alkali metal sulphates.

The bands at 1,635 cm^{-1} and 1,460 cm^{-1} can be assigned to carbonate species on the surface originating from preparation.

3.3 Monolith Sample

For wash-coating the monolith an appropriate slurry of the powder material was prepared (see Sect. 2.1). To exclude modifications of the storage properties during this preparation step, the dried slurry powder (500 °C, 1 h) was subjected to the cyclic test mode. Figure 6 allows a comparison of the SO_x storage behaviour of the dried slurry with the original powder sample. Both samples show a similar SO_2 removal profile but obviously the slurry has lost a certain part of its storage property during preparation and calcination. Analysis shows that there is a decrease of about 12% of the SO_x removal capacity within 8 h time-on-stream. The corresponding amount of stored sulphate drops from 20 to 18 wt.%.

Next, the wash-coated monolith core was examined. Different to the tests of the powder samples the temperature cycling started at 200 °C, because decreasing the temperature of the core from 600 °C down to 50 °C was not possible within reasonable time. Thus the duration of

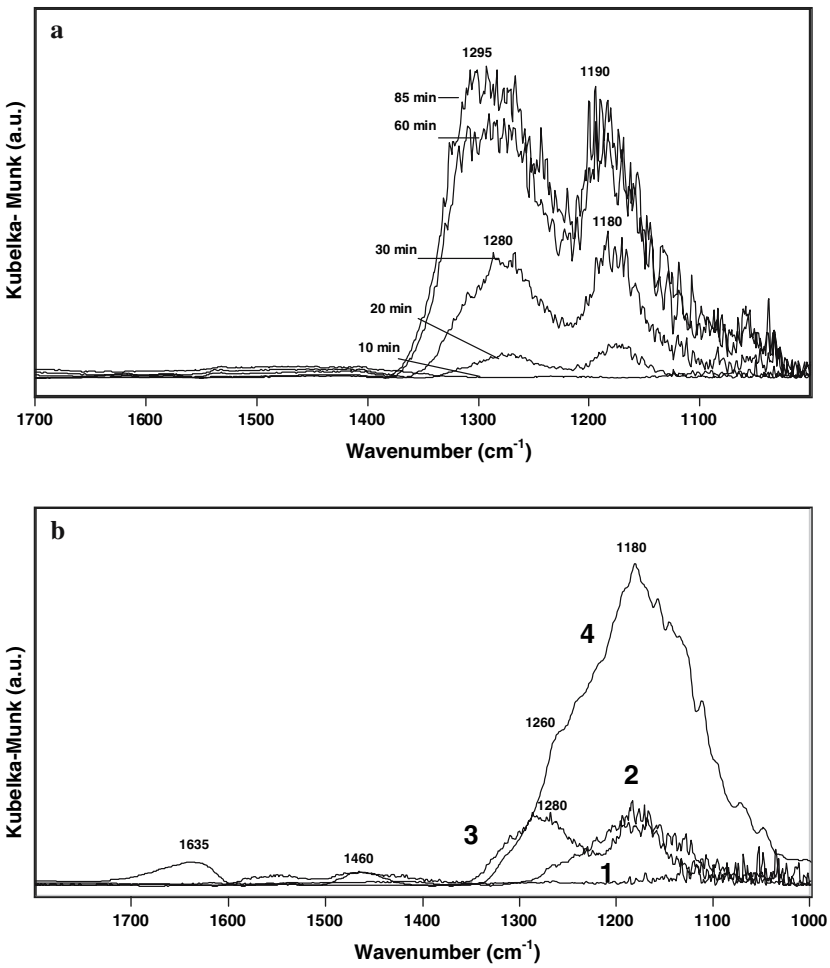

Fig. 5 In situ DRIFT spectra: (**a**) of MnO_x/Al_2O_3 during adsorption of SO_2 at 100 °C after indicated time-on-stream, feed: 200 ppm SO_2, 7.4% O_2, He; (**b**) comparison of (1) Al_2O_3, (2) Na/Al_2O_3, (3) MnO_x/Al_2O_3 and (4) $NaMnO_x/Al_2O_3$ after adsorption of SO_2 at 100 °C for 30 min; feed: 200 ppm SO_2, 7.4% O_2, balance He

four temperature cycles required a time of about 7 h. The gas velocity was increased to 4 L/min to ensure a comparable space velocity referring to the wash-coated powder volume.

Results of SO_2 storage of the monolith sample ($NaMnO_x/Al_2O_3$/cordierite) are shown for four temperature cycles, and for further three temperature cylces after intermediate shut-down overnight in Fig. 7a and b, respectively. Please, note that exit concentrations of SO_2 are plotted versus time-on-stream.

During the first three temperature cycles SO_2 has been completely stored. SO_2 breakthrough is observed after nearly 4 h time-on-stream. After 7 h time-on-stream, the amount of SO_x stored on the sample is still 93%; i.e. the accumulated sulphate amounts to about 20 wt.% referred to the weight of the supported powder material. This capacity is even slightly higher than found for the powdered slurry, but might be caused by the different temperature cycling range (50–600 °C for the powder and 200–600 °C for the monolith).

Continuation of the experiment after intermediate shut-down overnight (where the sample was flushed with N_2 at

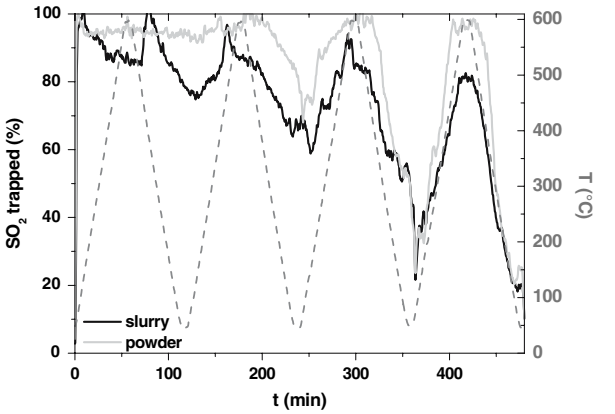

Fig. 6 SO_2 uptake on $NaMnO_x/Al_2O_3$. Comparison between powder and dried slurry. TPA/D in feed atmosphere from 50 to 600 °C (temperature ramp 10 K/min; intermediate cooling from 600 to 50 °C, dashed grey line, right axis), feed: 50 ppm SO_2. 6 vol.% O_2, 5 vol.% CO_2, 100 ppm NO, balance He

room temperature) revealed that the ability of the monolith to store SO_2 at low temperatures decreased continuously while at higher temperatures the storage of SO_2 still reached

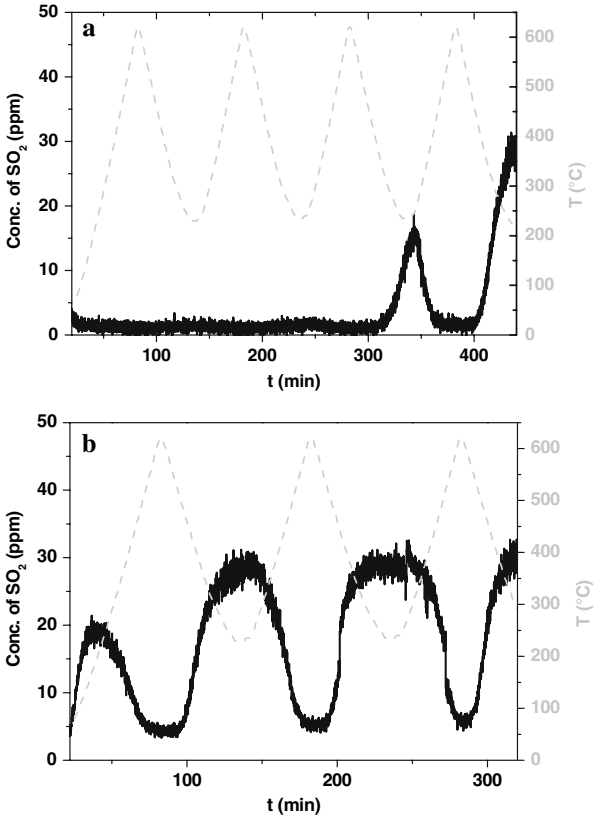

Fig. 7 SO_2 uptake on $NaMnO/Al_2O_3$ wash-coated on a cordierite core vs. time-on-stream with shut-down overnight. TPA/D in feed atmosphere from 200 to 600 °C (temperature ramp 10 K/min; intermediate cooling from 600 to 200 °C, dashed grey line, right axis), feed: 50 ppm SO_2. 6 vol.% O_2, 5 vol.% CO_2, 100 ppm NO, balance N_2. Four temperature cycles (1st day) (**a**) and three cycles (2nd day) (**b**)

a high level of 90% at 600 °C with only 5 ppm SO_2 release into the exit stream of initial 50 ppm (Fig. 7b). In summary, during 12 h time-on-stream about 80% of the offered SO_2 has been stored by the monolith, corresponding to about 23% sulphate referring to the wash-coated powder volume. This capacity roughly meets the requirements for SO_2 trapping between inspection intervals of passenger vehicles taking into account, that the actual SO_x concentration in exhaust gas streams is even lower than 50 ppm.

Onboard regeneration studies with an 1:3 (v/v) mixture of CO/H_2 to adjust the λ-value to 0.99 showed that about 69% of the stored SO_2 could be desorbed by this treatment. Full regeneration was not possible under the applied conditions.

4 Conclusions

It could be confirmed that hydrotalcite-derived Al_2O_3–MgO modified by MnO_x and Na can serve as SO_x trap materials with high capacity. However, thermal stability of hydrotalcites is limited, and, covering a temperature range up to 600 °C, they possess no advantages over non-hydrotalcite Al_2O_3–MgO or Al_2O_3. Modified by an amorphous MnO_x phase and Na both non-hydrotalcite Al_2O_3–MgO and Al_2O_3 showed high adsorption capacity for SO_2 with up to 20–23 wt.% sulphate formed during 8–12 h time-on-stream under temperature cycling between 50 and 600 °C. The formation of sulphate species on Mn, alkali metal and Al sites could be demonstrated by DRIFT measurements.

Preparation of a slurry from the most promising powder material $NaMnO_x/Al_2O_3$ and the wash-coating of a monolith cordierite core revealed nearly no change of the SO_x storage properties. This shows that up-scaling as well as application of the SO_x trap materials seem possible.

Acknowledgment The authors gratefully acknowledge financial support from the European Commission in the frame of the NANOSTRAP project (G3RD-CT2002-00793).

References

1. Takahashi N, Shinjoh H, Iijima T, Suzuki T, Yamazaki K, Yokota K, Suzuki H, Miyoshi N, Matsumoto S, Tanizawa T, Tanaka T, Tateishi S, Kasahara K (1996) Catal Today 27:63
2. Bögner W, Krämer M, Krutzsch B, Pischinger S, Voigtländer D, Wenninger G, Brogan M, Brisley R, Webster DE (1995) Appl Catal B: Environ 7:153
3. Engström P, Amberntsson A, Skolundh M, Fridell E, Smedler G (1999) Appl Catal B: Environ 22:241
4. Mahzoul H, Brilhac JF, Gilot P (1999) Appl Catal B: Environ 20:47
5. Amberntsson A, Westerberg B, Engström P, Fridell E, Skolundh M (1999) Stud Surf Sci Catal 126:317
6. Courson C, Khalfi A, Mahzoul H, Hodjati S, Moral N, Kiennemann A, Gilot P (2002) Catal Commun 3:471
7. Uy D, Wiegand KA, O'Neill AE, Dearth MA, Weber WH (2002) J Phys Chem B 106:387
8. Burch R (2004) Catal Rev 46:271
9. Huang HY, Long RQ, Yang RT (2001) Appl Catal B: Environ 33:127
10. Clacens J-M, Montiel R, Kochkar H, Figueras F, Guyon M, Beziat JC (2004) Appl Catal B: Environ 53:21
11. Limousy L, Mahzoul H, Brilhac JF, Garin F, Maire G, Gilot P (2003) Appl Catal B: Environ 45:169
12 Rohr F, Peter SD, Lox E, Kögel M, Sassi A, Juste L, Rigaudeau C, Belot G, Gélin P, Primet M (2005) Appl Catal B: Environ 56:201
13. Schreier E, Eckelt R, Richter M, Fricke R (2005) Catal Commun 6:409
14. Limousy L, Mahzoul H, Brilhac JF, Gilot P, Garin F, Maire G (2003) Appl Catal B: Environ 42:237
15. Dathe H, Sedlmair C, Jentys A, Lercher JA (2004) In: van Steen E et al. (ed) Proc 14th Int Zeolite Conf, Cape Town, 25–30 April 2004, p 3003
16. Dathe H, Haider P, Jentys A, Schreier E, Fricke R, Lercher JA (2006) Phys Chem Chem Phys 8:1601
17. Centi G, Perathoner S (2006) Catal Today 112:174
18. Schreier E, Eckelt R, Richter M, Fricke R (2006) Appl Catal B: Environ 65:249

19. Hodjati S, Petit C, Pitchon V, Kiennemann A (2001) Appl Catal B: Environ 30:247
20. de Wilde J, Das AK, Heynderickx GH, Marin GB (2001) Ind Eng Chem Res 40:119
21. Schneider WF, Li J, Hass KC (2001) J Phys Chem B 105:6972
22. Li L, King DL (2005) Ind Eng Chem Res 44:168
23. Tikhomirov K, Kröcher O, Elsener M, Widmer M, Wokaun A (2006) Appl Catal B: Environ 67:160
24. Fornasari G, Trifirò F, Vaccari A, Prinetto F, Ghiotti G, Centi G (2002) Catal Today 75:421
25. Basile F, Fornasari G, Livi M, Tinti F, Trifirò F, Vaccari A (2004) Topics Catal 30:223
26. Fornasari G, Glöckler R, Livi M, Vaccari A (2005) Appl Clay Sci 29:258
27. Yu JJ, Jiang Z, Zhu L, Hao ZP, Xu ZP (2006) J Phys Chem B 110:4291
28. Corma A, Palomares AE, Rey F, Márquez F (1997) J Catal 170:140
29. Palomares AE, López-Nieto JM, Lázaro FJ, López A, Corma A (1999) Appl Catal B: Environ 20:257
30. Centi G, Fornasari G, Gobbi C, Livi M, Trifirò F, Vaccari A (2002) Catal Today 73:287
31. Centi G, Perathoner S (2007) Appl Catal B: Environ 70:172
32. Polato CMS, Henriques CA, Neto AA, Monteiro JLF (2005) J Mol Catal A: Chem 241:184
33. Cantú M, López-Salinas E, Valente JS (2005) Environ Sci Technol 39:9715
34. Rey F, Fornés V, Rojo J.M. (1992) J Chem Soc Faraday Trans 88:2233
35. Di Cosimo JI, Diez VK, Xu M, Iglesia E, Apesteguia CR (1998) J Catal 178:499
36. Richter M, Berndt H, Eckelt R, Schneider M, Fricke R (1999) Catal Today 54:531
37. Güldür C, Doğu G, Doğu T (2001) Chem Eng Proc 40:13
38. Kijlstra WS, Biervliet M, Poels EK, Bliek A (1998) Appl Catal B: Environ 16:327